Supplemental Material to "Unveiling the Two-Proton Halo Character of ^{17}Ne: Exclusive Measurement of Quasi-free Proton-Knockout Reactions"

C. Lehr,[1] F. Wamers,[1,2] F. Aksouh,[1,2,*] Yu. Aksyutina,[2] H. Álvarez-Pol,[3] L. Atar,[1,2] T. Aumann,[1,2,4,†] S. Beceiro-Novo,[3,‡] C.A. Bertulani,[5] K. Boretzky,[2] M.J.G. Borge,[6] C. Caesar,[1,2] M. Chartier,[7] A. Chatillon,[2] L.V. Chulkov,[2,8] D. Cortina-Gil,[3] P. Díaz Fernández,[3,9] H. Emling,[2] O. Ershova,[2,10] L.M. Fraile,[11] H.O.U. Fynbo,[12] D. Galaviz,[6] H. Geissel,[2] M. Heil,[2] M. Heine,[1] D.H.H. Hoffmann,[1] M. Holl,[1,2,9] H.T. Johansson,[9] B. Jonson,[9] C. Karagiannis,[2] O.A. Kiselev,[2] J.V. Kratz,[13] R. Kulessa,[14] N. Kurz,[2] C. Langer,[2,10,§] M. Lantz,[9,¶] T. Le Bleis,[2] R. Lemmon,[15] Yu.A. Litvinov,[2] B. Löher,[2,1] K. Mahata,[2,16] J. Marganiec-Galązka,[1,2,**] C. Müntz,[10] T. Nilsson,[9] C. Nociforo,[2] W. Ott,[2,††] V. Panin,[2,1] S. Paschalis,[2,7,‡‡] A. Perea,[6] R. Plag,[2,10] R. Reifarth,[10,2] A. Richter,[1] K. Riisager,[12] C. Rodriguez-Tajes,[3] D. Rossi,[1,2,13] D. Savran,[2] H. Scheit,[1] G. Schrieder,[1] P. Schrock,[1] H. Simon,[2] J. Stroth,[10,2] K. Sümmerer,[2] O. Tengblad,[6] H. Weick,[2] and C. Wimmer[10,2]

[1] *Technische Universität Darmstadt, Department of Physics, D–64289 Darmstadt, Germany*
[2] *GSI Helmholtzzentrum für Schwerionenforschung GmbH, D–64291 Darmstadt, Germany*
[3] *Instituto Galego de Física de Altas Enerxias, Universidade de Santiago de Compostela, ES–15782 Santiago de Compostela, Spain*
[4] *Helmholtz Research Academy Hesse for FAIR, D–64289 Darmstadt, Germany*
[5] *Texas A&M University-Commerce, Commerce, USA*
[6] *Instituto de Estructura de la Materia, CSIC, ES–28006 Madrid, Spain*
[7] *Department of Physics, University of Liverpool, Liverpool L69 3BX, United Kingdom*
[8] *NRC Kurchatov Institute, RU–123182 Moscow, Russia*
[9] *Department of Physics, Chalmers Tekniska Högskola, SE–41296 Göteborg, Sweden*
[10] *Goethe Universität Frankfurt, Department of Physics, D–60438 Frankfurt am Main, Germany*
[11] *Grupo de Física Nuclear* & IPARCOS, Universidad Complutense de Madrid, CEI Moncloa, ES–28040 Madrid, Spain
[12] *Department of Physics and Astronomy, University of Aarhus, DK–8000 Aarhus, Denmark*
[13] *Institut für Kernchemie, Johannes Gutenberg-Universität Mainz, D–55122 Mainz, Germany*
[14] *Instytut Fizyki, Uniwersytet Jagielloński, PL–30-059 Kraków, Poland*
[15] *Nuclear Physics Group, STFC Daresbury Lab, Warrington WA4 4AD, Cheshire, UK*
[16] *Nuclear Physics Division, Bhabha Atomic Research Centre, Trombay, Mumbai-400 085, India*

(Dated: December 6, 2021)

Previous work

^{17}Ne ($J^\pi = 1/2^-$) has seven neutrons and ten protons, β^+-decays towards ^{17}F ($T_{1/2} = 109$ ms), and is loosely bound. The proton separation energies are $S_p = 1464(5)$ keV and $S_{2p} = 933.1(6)$ keV, while its neutron separation energy is $S_n = 15558(20)$ keV [1]. The $p-p$ pairing energy estimated as the difference between S_p of the second proton and that of the first proton is -2005(11) keV. ^{15}O ($J^\pi = 1/2^-$) is essentially strongly bound, $S_p = 7296.8(5)$ keV and $S_{2p} = 14847.3(5)$ keV, with about ten times weaker $p-p$ pairing energy. This is an indication that ^{17}Ne can be described as a ^{15}O core plus two valence protons, predominantly in a mixture of $(1s_{1/2})^2$ and $(0d_{5/2})^2$ configurations, coupled to $J^\pi = 0^+$. With its binary subsystems ^{16}F and $p-p$ unbound, ^{17}Ne is a *Borromean* nucleus – such as the classical two-neutron halo nuclei ^{6}He and ^{11}Li – so that it has been valued as a good candidate for a two-proton halo nucleus [2].

Evidence for a proton halo in ^{17}Ne in terms of a possibly dominating $(1s_{1/2})^2$ configuration was found in measurements of interaction cross sections for $A = 17$ high energy beams [3]. Calculations of the interaction cross section by using a Hartree-Fock-type wave function and the Glauber model yielded no conclusion on the ^{17}Ne halo [4]. Analysis of the reaction cross sections measured using ^{17}Ne 64 and 42 MeV/nucleon beams revealed a halo-like dilute tail in the density distribution, consistent with a dominant $(1s_{1/2})^2$ configuration for valence protons [5]. But recent calculations reproducing experimental measurements, including the results of Ref. [5], such as binding energies, matter

* *Present address:* Department of Physics and Astronomy, College of Science, King Saud University, P.O. Box 2455, 11451 Riyadh, KSA
† *E-mail:* Thomas.Aumann@tu-darmstadt.de
‡ *Present address:* NSCL, Michigan State University, East Lansing, Michigan 48824, USA
§ *Present address:* FH Aachen University of Applied Science, D–52066 Aachen, Germany
¶ *Present address:* Department of Physics and Astronomy, Uppsala University, SE–751 20 Uppsala, Sweden
** *Present address:* National Centre for Nuclear Research, Radioisotope Centre POLATOM, 05-400 Otwock, Poland
†† deceased
‡‡ *Present address:* Department of Physics, University of York, York, YO10 5DD, UK

radii, charge radii and nuclear matter density distribution resulted in about 20% [6] for the occupation probability of the $(1s_{1/2})^2$ orbital.

The experimental momentum distribution of ^{15}O and the two-proton-removal cross section obtained in fragmentation of ^{17}Ne was explained assuming $P((1s_{1/2})^2) = 60 - 100\%$ [7, 8]; however, that measurement was not exclusive to proton-removal from the ^{17}Ne halo. Calculations within the framework of a three-cluster generator-coordinate model concluded on no proton halo in ^{17}Ne [9], and calculations using a density-dependent contact pairing interaction between the valence protons and the (^{15}O$+p+p$)-modelled ^{17}Ne resulted to $P((1s_{1/2})^2) = 15.2\%$, $P((0d_{5/2})^2) = 75.2\%$, and $P((0d_{3/2})^2) = 3.8\%$ [10, 11].

A $^{15}\mathrm{O} + p + p$ three-body model was also used to calculate Thomas-Ehrman shifts for ^{17}Ne and ^{17}N [12–14]. Both articles agree on a $P((1s_{1/2})^2)$ value of in between 40-50%. As mentioned in Ref. [14], the computed three-body Thomas-Ehrman shifts are meaningful, albeit relatively inaccurate. Coulomb energies for mirror nuclei ^{17}Ne and ^{17}N were also computed in other models [15–17]. While the predominance of a $(1s_{1/2})^2$ configuration was stated in Ref. [15], the two other publications agree on $P((1s_{1/2})^2) = 24(3)\%$.

The ^{17}Ne magnetic dipole moment measured by collinear laser spectroscopy could be reproduced with a theoretical model assuming $P((1s_{1/2})^2) = 24\%$, $P((0d_{5/2})^2) = 69\%$, and $P((0d_{3/2})^2) = 7\%$ [18]. High-precision charge-radii measurements using collinear laser spectroscopy for ^{17,18,19}Ne of 3.04(2), 2.97(2), and 3.01(1) fm [19] do not support a pronounced halo for ^{17}Ne. A theoretical analysis using the fermionic molecular dynamics (FMD) approach has been employed to relate the radius to the s^2 occupation. By slightly changing the strength of the spin-orbit force, the charge radius and s^2 occupation have been tuned arriving at an allowed region between 38% and 46% s^2 contribution corresponding to a charge-radius change within the experimental uncertainty. Thereby, it was assumed that only the two valence protons contribute [19].

The first-forbidden β^+-decay of ^{17}Ne into the first excited state of ^{17}F was measured by Borge *et al.* [20]. This decay is by a factor two faster than the corresponding mirror decay, an effect which was explained by assuming the $1s_{1/2}$ proton orbit to have a large spatial (halo-like) extent, but only a small admixture to the ^{17}Ne ground state [20]. The asymmetry in $\beta\pm$ decays of ^{17}Ne and ^{17}N was explained by charge-related differences in their ground-state wavefunctions by Millener *et al.* [21]. However, authors of Ref. [9] argue that the first-forbidden β-decays of the ^{17}Ne and ^{17}N ground states are independent of possible halo effects in the initial or final nuclei.

Ref.	Year	Exp./Theo.	Method	$P(s^2)/(P(s^2)+P(d^2))$
[20]	1993	Exp	Beta-decay spectroscopy	-
[3]	1994	Exp	Interaction cross section measurements	-
[2]	1995	Theo	Three-body model: CSF - SSC(C)	0.50
[2]	1995	Theo	Three-body model: CSF - Gaussian	0.27
[9]	1996	Theo	Microscopic calculation	“no proton halo”
[21]	1997	Theo	Calculation of nuclear matrix elements	-
[4]	1997	Theo	Glauber: reaction cross section and matter radii	“proton halo in ^{17}Ne is still not conclusive”
[15]	1998	Theo	Coulomb mass shift	1.00
[7]	2003	Exp	^{15}O $p_{\|\|}$ + proton-removal cross section	“large”
[12, 13]	2004	Theo	Coulomb displacement energy to ^{17}N	0.50
[14]	2004	Theo	Three-body model: Thomas Ehrmann shifts	-
[18]	2005	Exp	^{17}Ne magnetic dipole moment	0.26
[17]	2006	Theo	Coulomb energy parametrisation	-
[19]	2008	Exp	^{17}Ne mass and charge radii	0.42
[10, 11]	2010	Theo	Three-body model, including Coulomb	0.17
[5]	2010	Exp	Reaction cross section measurement	“dominant s”
[6]	2013	Theo	Relativistic mean field theory	0.33
This work	2021	Exp	Exclusive (p,2p) knockout, Momentum distribution	0.34(5)
This work	2021	Exp	Exclusive (p,2p) knockout, Population of states	0.36(5)

TABLE I. Compilation of experimental and theoretical results on the s-d content in the ^{17}Ne valence-nucleon wavefunction.

Measurement of the energy spectrum of ^{16}F

^{16}F is produced from ^{17}Ne by one-proton $(p, 2p)$ quasi-free knockout reactions. The two scattered protons are detected at large angles around 45°. The decay products of the unbound ^{16}F, *i.e.*, ^{15}O and p are detected in coincidence in forward direction and momentum analyzed. From their measured momenta, the ^{16}F relative energy is determined by using the invariant-mass method. The resolution for the ^{15}F$-p$ relative-energy spectrum is determined by the multiple scattering of the charged particles in detector material and gases. The main contribution to the resolution stems from the proton. Figure 6 shows the simulated response for $E_{\rm fp}$ for the two decay energies 1.05 and 4.05 MeV. The corresponding resolutions are $\sigma = 0.11$ MeV and $\sigma = 0.25$ MeV, respectively.

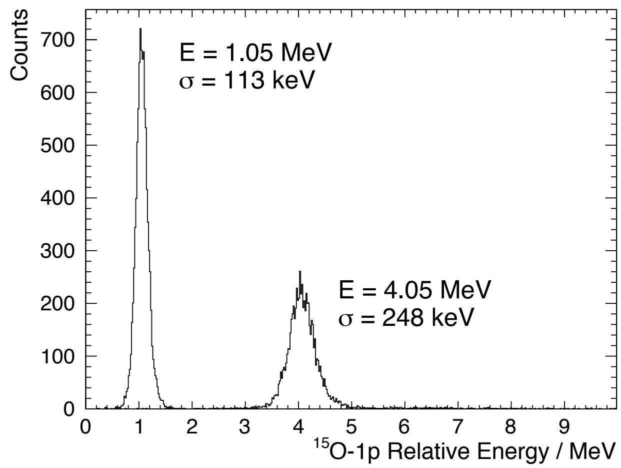

FIG. 6. Experimental response function to a given decay energy as obtained from simulations. Examples are shown for a 1 MeV and a 4 MeV line. The relative-energy spectrum has been calculated from the momenta of the decay products ^{15}O and p in the same way as for the experimental data. Detector resolutions and multiple scattering in the various materials have been taken into account.

The excitation energy of ^{16}F is the sum of the relative energy between the decay fragments and the energy released by additional γ-decays. Photons are detected by the Crystal Ball 4π NaI array surrounding the target. Figure 7 (left) shows the γ-spectrum measured in coincidence in the ^{17}Ne$(p,2p)^{16}$F$^* \rightarrow ^{15}$O$+p$ reaction. A peak-like structure is observed at an energy of around 5 MeV. The arrows indicate expected transitions from the known excited states as indicated in the level scheme in the inset. The corresponding relative-energy spectrum measured in coincidence is shown on the right in Figure 7. A broad distribution of energies is visible with most intensity located around 3 MeV. These decays result from high-lying excited states of ^{16}F after knockout of a more deeply bound proton from the p shell of the core, while the halo protons act as spectators. One of the halo protons couples to the remaining ^{14}N forming an excited ^{15}O state which γ decay to the ^{15}O ground state, while the second halo proton is emitted in forward direction. The γ-spectrum shows a significant background which stems from the background produced by the scattered protons, and in the low-energy region left of the peak also from incomplete γ-energy detection. The resulting background spectrum for $E_{\rm fp}$ has been obtained by gating on events in the γ-spectrum with energies larger than the peak region. This background spectrum has been subtracted to obtain the spectrum shown on the right. The remaining spectrum, corresponding to the relative-energy distribution in coincidence with γ-transitions (right frame in Fig. 7), has been then subtracted from the total $E_{\rm fp}$ spectrum before that has been analyzed in terms of population of the low-lying s and d states as shown in Fig. 3 of the main text.

The line shapes of the four low-lying resonances are described by the Breit-Wigner formula,

$$d_\sigma/dE_{fp} \propto \frac{\Gamma_0(E_{fp})}{(E_r - E_{fp})^2 + \frac{1}{4}\Gamma_0(E_{fp})^2},$$

with the resonance energy E_r and width $\Gamma_0(E_{fp}) = \Gamma_{\rm exp} P_l(E_{fp})/P_l(E_{\rm res})$. The penetrabilities $P_l(E_{\rm res})$ contain the regular and irregular Coulomb wave functions and the channel radius R which has been chosen as $R = 5$ fm. Resonance parameters have been taken from Ref. [22]. Since the discussed resonances are very narrow compared to the experimental resolution, resonance shift factors are negligible and the shapes are rather insensitive to the choice of the channel radius. Additional uncertainties due to the details of the line shape used in the fit are thus negligible compared to the experimental uncertainties for the extracted s to d cross-section ratio.

^{16}F Momentum distributions after proton knockout

The momentum distributions of the unbound ^{16}F after proton knockout from ^{17}Ne can be calculated as the sum of the momenta of the decay products p and ^{15}O measured in forward direction and analyzed with the ALADIN dipole

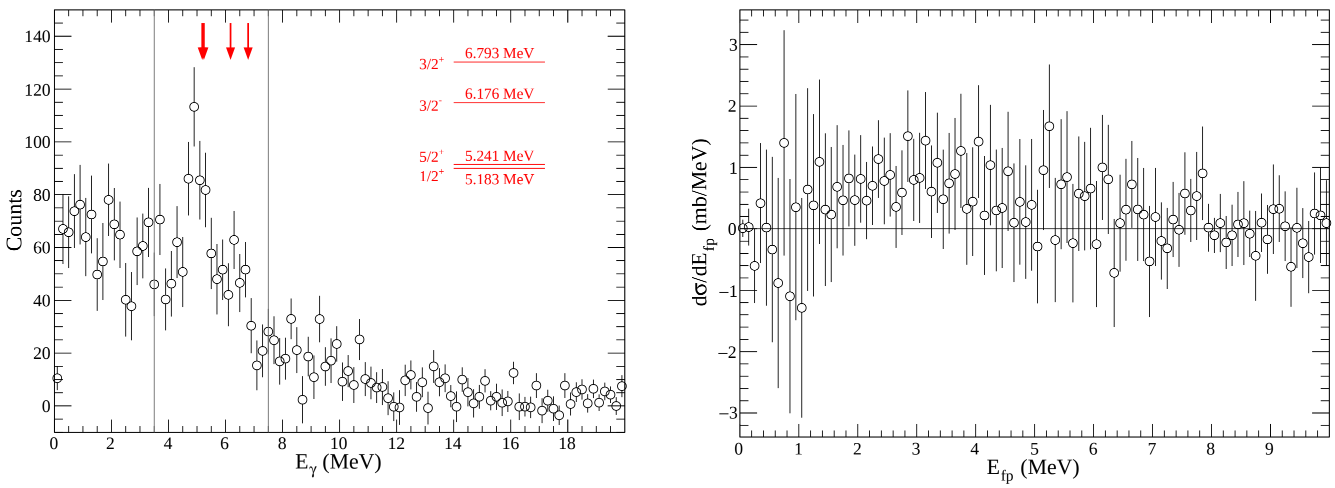

FIG. 7. Left: Gamma-spectrum for the reaction channel ^{17}Ne$(p, 2p)^{15}$O. The energies of known γ-transitions in the peak region around 5 MeV are indicated by arrows (see also level scheme indicated as inset). Right: Relative-energy spectrum in coincidence with γ-transitions in the energy window as indicated by the vertical lines in the spectrum on the left. The relative-energy spectrum has been corrected for background contributions by subtracting a spectrum obtained by gating on the high-energy part of the γ-spectrum, which has been normalized assuming a smoothly rising background towards lower energies.

magnet. The transverse components p_x and p_y in cartesian coordinates are obtained by the position measurements of p and ^{15}O behind the target and their tracking through the ALADIN magnet field, as sketched in Fig. 1 of the main text. The used coordinate system has the z axis along the incoming beam direction, which is determined on an event-by-event basis by two position measurements in front of the target. The resulting distributions are shown in Fig. 8 for the two transverse components. The curves show the calculated distributions for s (long-dashed, blue) and d (dashed, red) states and their sum (solid curve, black). The normalisation of the theoretical distributions was obtained by χ^2-minimisation to the data, where the individual intensities were varied freely in a simultaneous fit to the x and y distributions. Figure 9 shows the same comparison for the restricted relative-energy region $0 < E_{fp} < 1.2$ MeV, resulting in a suppressed contribution of the higher-lying d states, as expected.

Since these momentum distributions reflect the intrinsic momentum distributions of the knocked-out protons, they are sensitive to the angular momentum l. The shape of the wavefunction is different for different l values, in particular also in the asymptotic behaviour due to the different centrifugal barriers. Due to the large centrifugal barrier for the $l = 2$ state, the asymptotic fall-off of the d-wavefunction is much faster compared to the s state with the same binding energy. The resulting rms radii of the two single-particle wavefunctions are 4.23 fm and 3.46 fm for the s and d case if normalized to $S = 1$, respectively. The halo-like s-wave density results in a much more narrow momentum distribution. While the spatially more compact d-wave density results in a broad distribution in momentum space. The radii compare to a rms radius of the core of 2.64 fm, resulting in differences $\Delta r = r_{halo} - r_{core}$ of 1.6 fm and 0.8 fm for the pure s^2 and d^2 states respectively. Our result for the $s^2/(s^2 + d^2)$ ratio of 0.35(5) corresponds to a difference of radii of the valence-nucleon density and the core of 1.1 fm.

The strong sensitivity of the momentum distribution to the l value is used to determine the $s^2/(s^2 + d^2)$ ratio by comparing to theoretical calculations based on Woods-Saxon wavefunctions. The slight distortion due the reaction mechanism is thereby taken into account with the Glauber reaction theory [23]. The Glauber theory is well established in electron-induced knockout reactions at high energy and large momentum transfer. The situation is very similar in $(p, 2p)$ at beam energies as used here, resulting in large momentum transfer and high energy of the scattered protons of around 250 MeV. The $(p, 2p)$ reaction and the theoretical treatment has been benchmarked in a previous experiment using a ^{12}C beam against high-quality (e, e') data from NIKHEF. Good agreement is found in terms of spectroscopic factors as well as the shape of momentum distributions is concerned [24].

[1] M. Wang, W. J. Huang, F. G. Kondev, G. Audi, S. Naimi, Chinese Physics C **3**, 030003 (2021).
[2] M. V. Zhukov and I. J. Thompson, Phys. Rev. C **52**, 3505 (1995).
[3] A. Ozawa, T. Kobayashi, H. Sato, D. Hirata, I. Tanihata, O. Yamakawa, K. Omata, K. Sugimoto, D. Olson, W. Christie, and H. Wieman, Physics Letters B **334**, 18 (1994).

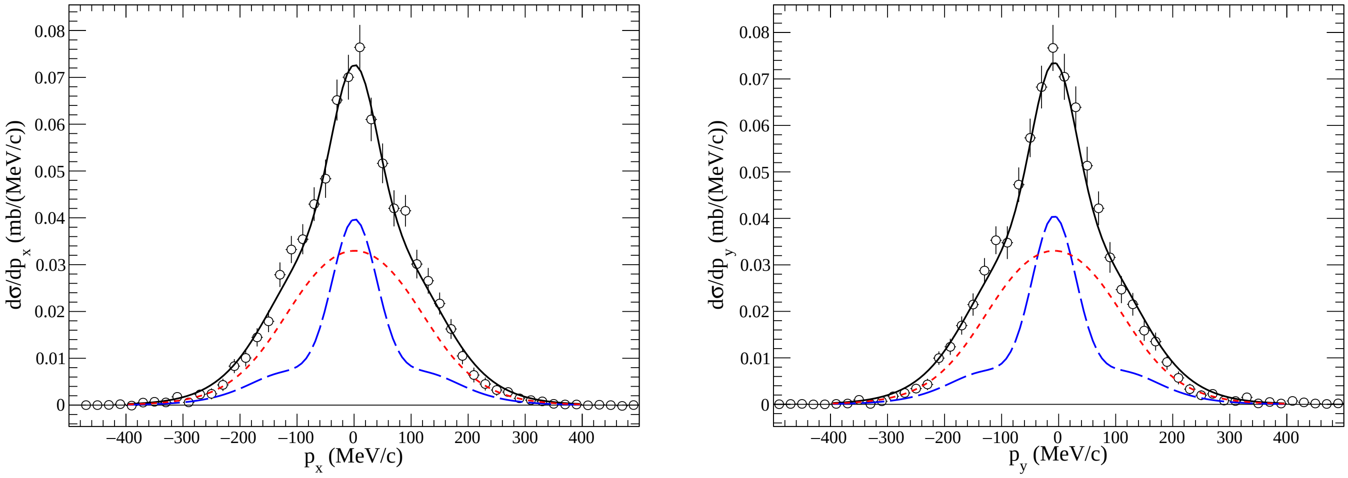

FIG. 8. Transverse momentum distributions of the recoiling ^{16}F fragment (after one-proton knockout on a ^{17}Ne beam) reconstructed from the measured momenta of ^{15}O and p. The left (right) frame shows the distribution in the cartesian coordinates x (y) in a plane perpendicular to the beam axis. The curves show the calculated distributions for s (long-dashed, blue) and d (dashed, red) states and their sum (solid curve, black). The normalisation of the theoretical distributions was obtained by χ-square minimisation to the data, where the individual intensities were varied freely in a simultaneous fit to the x and y distributions.

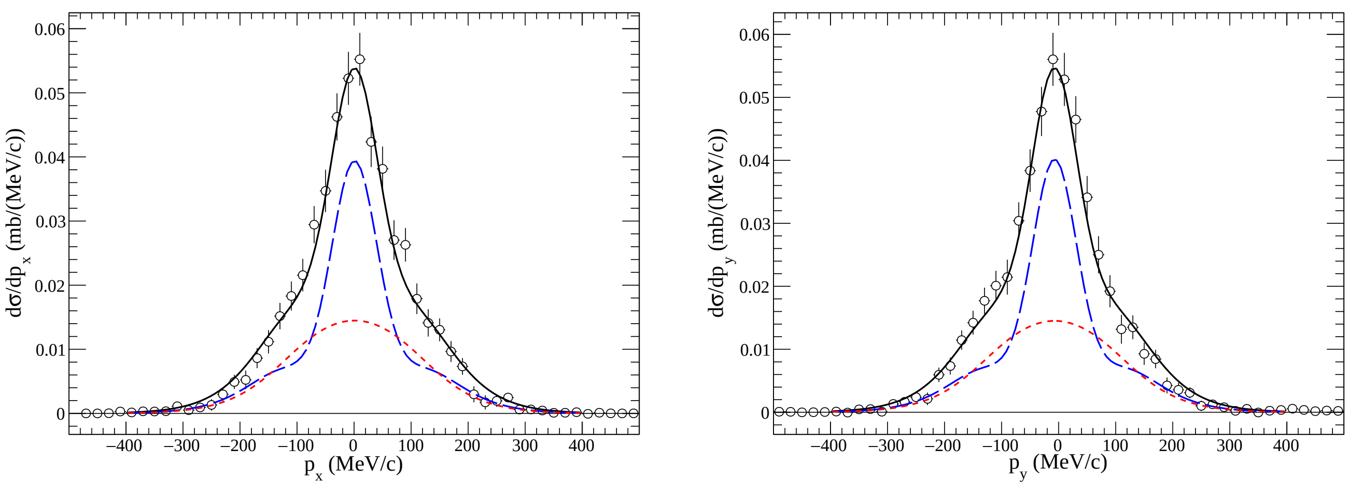

FIG. 9. Same as Fig. 8 for the restricted relative-energy region $0 < E_{fp} < 1.2$ MeV, resulting in a suppressed contribution of the higher-lying d states.

[4] H. Kitagawa, N. Tajima, and H. Sagawa, Zeitschrift für Physik A **358**, 381 (1997).

[5] K. Tanaka, M. Fukuda, M. Mihara, M. Takechi, D. Nishimura, T. Chinda, T. Sumikama, S. Kudo, K. Matsuta, T. Minamisono, T. Suzuki, T. Ohtsubo, T. Izumikawa, S. Momota, T. Yamaguchi, T. Onishi, A. Ozawa, I. Tanihata, and T. Zheng, Phys. Rev. C **82**, 044309 (2010).

[6] S.-S. Zhang, E.-G. Zhao, and S.-G. Zhou, The European Physical Journal A **49**, 10.1140/epja/i2013-13077-8 (2013).

[7] R. Kanungo, M. Chiba, S. Adhikari, D. Fang, N. Iwasa, K. Kimura, K. Maeda, S. Nishimura, Y. Ogawa, and T. Ohnishi, Physics Letters B **571**, 21 (2003).

[8] R. Kanungo, M. Chiba, B. Abu-Ibrahim, S. Adhikari, D. Q. Fang, N. Iwasa, K. Kimura, K. Maeda, S. Nishimura, T. Ohnishi, A. Ozawa, C. Samanta, T. Suda, T. Suzuki, Q. Wang, C. Wu, Y. Yamaguchi, K. Yamada, A. Yoshida, T. Zheng, and I. Tanihata, European Physics Journal A **25**, 327 (2005).

[9] N. Timofeyuk, P. Descouvemont, and D. Baye, Nuclear Physics A **600**, 1 (1996).

[10] T. Oishi, K. Hagino, and H. Sagawa, Phys. Rev. C **82**, 024315 (2010).

[11] T. Oishi, K. Hagino, and H. Sagawa, Phys. Rev. C **82**, 069901 (2010).

[12] L. V. Grigorenko, I. G. Mukha, and M. V. Zhukov, Nuclear Physics A **713**, 372 (2003).

[13] L. V. Grigorenko, I. G. Mukha, and M. V. Zhukov, Nuclear Physics A **740**, 401 (2004).

[14] E. Garrido, D. V. Fedorov, and A. S. Jensen, Phys. Rev. C **69**, 024002 (2004).
[15] S. Nakamura, V. G. aes, and S. Kubono, Physics Letters B **416**, 1 (1998).
[16] H. Fortune and R. Sherr, Physics Letters B **503**, 70 (2001).
[17] H. T. Fortune, R. Sherr, and B. A. Brown, Phys. Rev. C **73**, 064310 (2006).
[18] W. Geithner, B. A. Brown, K. M. Hilligsøe, S. Kappertz, M. Keim, G. Kotrotsios, P. Lievens, K. Marinova, R. Neugart, H. Simon, and S. Wilbert, Phys. Rev. C **71**, 064319 (2005).
[19] W. Geithner, T. Neff, G. Audi, K. Blaum, P. Delahaye, H. Feldmeier, S. George, C. Guénaut, F. Herfurth, A. Herlert, S. Kappertz, M. Keim, A. Kellerbauer, H.-J. Kluge, M. Kowalska, P. Lievens, D. Lunney, K. Marinova, R. Neugart, L. Schweikhard, S. Wilbert, and C. Yazidjian, Phys. Rev. Lett. **101**, 252502 (2008).
[20] M. J. G. Borge, J. Deding, P. G. Hansen, B. Jonson, G. Martinez-Pinedo, P. Møller, G. Nyman, A. Poves, A. Richter, K. Riisager, and O. Tengblad, Physics Letters B **317**, 25 (1993).
[21] D. J. Millener, Phys. Rev. C **55**, R1633 (1997).
[22] I. Stefan, F. de Oliveira Santos, O. Sorlin, T. Davinson, M. Lewitowicz, G. Dumitru, J. C. Angélique, M. Angélique, E. Berthoumieux, C. Borcea, R. Borcea, A. Buta, J. M. Daugas, F. de Grancey, M. Fadil, S. Grévy, J. Kiener, A. Lefebvre-Schuhl, M. Lenhardt, J. Mrazek, F. Negoita, D. Pantelica, M. G. Pellegriti, L. Perrot, M. Ploszajczak, O. Roig, M. G. Saint Laurent, I. Ray, M. Stanoiu, C. Stodel, V. Tatischeff, and J. C. Thomas, Phys. Rev. C **90**, 014307 (2014).
[23] T. Aumann, C. A. Bertulani, and J. Ryckebusch, Phys. Rev. C **88**, 064610 (2013).
[24] V. Panin, J. Taylor, S. Paschalis, F. Wamers, Y. Aksyutina, H. Alvarez-Pol, T. Aumann, C. Bertulani, K. Boretzky, C. Caesar, M. Chartier, L. Chulkov, D. Cortina-Gil, J. Enders, O. Ershova, H. Geissel, R. Gernhäuser, M. Heil, H. Johansson, B. Jonson, A. Kelić-Heil, C. Langer, T. Le Bleis, R. Lemmon, T. Nilsson, M. Petri, R. Plag, R. Reifarth, D. Rossi, H. Scheit, H. Simon, H. Weick, and C. Wimmer, Physics Letters B **753**, 204 (2016).